



## **PREPARATION, TECHNIQUES AND TOOLS USED FOR INVESTIGATING GLASSES : AN OVERVIEW**

**PRIYA MURUGASEN<sup>\*</sup>, SURESH SAGADEVAN<sup>a</sup> and DEEPA SHAJAN<sup>b</sup>**

Department of Physics, Saveetha Engineering College, Thandalam, CHENNAI – 602105 (T.N.) INDIA

<sup>a</sup>Department of Physics, Sree Sastha Institute of Engineering and Technology,  
CHENNAI – 600123 (T.N.) INDIA

<sup>b</sup>Veltech Hightech Engineering College, Avadi, CHENNAI – 600052 (T.N.) INDIA

### **ABSTRACT**

This paper describes preparation of glasses by melt quench method and experimental techniques employed in the characterization of glasses. Characterization techniques such as X-ray Diffraction technique (XRD), Fourier Transform Infrared spectroscopy (FTIR); thermal, UV analysis, microhardness and dielectric studies and fluorescence spectroscopy etc. is described in detail. In addition, thermal poling and Z-scan technique experimental methods are discussed in this paper.

**Key words:** XRD, FTIR, Thermal, Microhardness, Fluorescence spectroscopy, Z-Scan technique.

### **INTRODUCTION**

Characterization techniques are important for researchers as these are the basic tools in identifying the structure and thereby properties of materials synthesized, which help in determining whether the designed materials are suitable for particular applications. We present the preparation and the experimental techniques to find out the structural, thermal, linear and nonlinear optical properties of glasses.

The characterization of a material can be defined as a complete description of its physical and chemical properties. A thorough and extensive characterization of a glass is very difficult, because it requires a variety of tests using a number of sophisticated instruments and an accurate analysis of the results of these tests and their confirmations. The use of instrumentation is an exciting and fascinating part of any analysis that interacts with all the areas of chemistry and with many other fields of pure and applied sciences. In most of the cases of chemical analysis, a signal is produced, which reflects the chemical or physical

---

\* Author for correspondence; E-mail: priyam7373@gmail.com

property of a chemical system. The present paper deals with the description of various characterization techniques and methods of preparation of glasses.

### **Glass preparation**

Most common glass preparation techniques in glass research are melt quench method, chemical vapor deposition and sol gel method. Bulk glasses in this research were prepared using melt quenching method. Melt quenching technique was the first glass preparation technique used in glass industry as well as in research field, before chemical vapour deposition and sol gel technique<sup>1,2</sup>. One of the important features of the melt quenching technique is the flexibility of preparing a large number of compositions of glass of silicate, borate, phosphate, oxide or non oxide systems. The doping or codoping of different types of active ions is quiet easy using this method. Compared to other glass preparation methods, the disadvantage is that the lack of purity of the prepared glass sample. In order to avoid contamination, the crucibles made of noble metals like Gold, Platinum etc can be used.

### **Melt quench method**

The glass starting materials were weighed using electronic balance after batch calculation. The glass batch was melted in a platinum crucible at 800°C and cast into a rectangular brass/steel mold at room temperature. All the melting processes were done using an electric furnace as shown in Fig. 1. Each glass sample was immediately transferred to an annealing furnace at 300°C and slowly cooled to room temperature<sup>3-5</sup>. These samples were then polished using various grades of silicon carbide powder for obtaining parallel, smooth and clear surface for experiment. The thickness of the glass specimens was measured using a digital micrometer gauge.



**Fig. 1: Furnace used for melt quenching**

## The glass transition

Glass formation is a matter of bypassing the process of crystallization<sup>1,6-9</sup> and almost all materials can, be prepared as amorphous solids by quick cooling. The rate of cooling varies enormously from material to material. When glass is made, the material is quickly cooled from a supercooled liquid, an intermediate state between liquid and glass. To become an amorphous solid, the material is cooled, below a critical temperature called the glass-transition temperature. The newly formed amorphous structure is not as organized as a crystal, but it is more organized than a liquid.

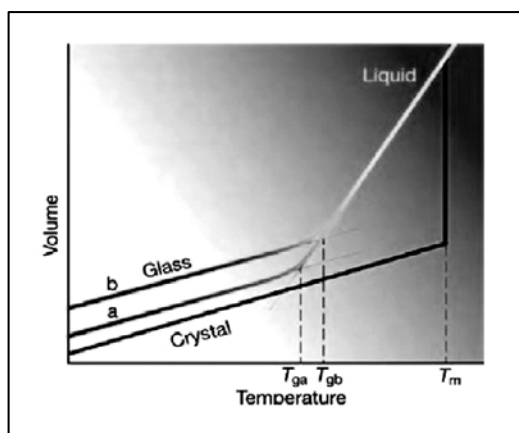


**Fig. 2: V-T Diagram showing glass formation**

In the process of glass transition, it is important to plot the behavior of amorphous materials, from the super cooled state to glass, in a V-T diagram [Fig. 2]. Here, temperature is plotted in the x-axis and the volume/enthalpy occupied by the material is plotted along the y-axis, where temperature  $T_m$  is the melting point, and  $T_g$  is the glass transition temperature. The glass transition occurs when the supercooled liquid freezes into an amorphous solid with no abrupt discontinuity in volume, near the glass transition temperature. The glass transition temperature  $T_g$  is not as sharply defined as  $T_m$ ;  $T_g$  shifts towards lower temperature when the cooling rate is reduced. The reason for this phenomenon is the steep temperature dependence of the molecular response with time.  $T_g$  also varies with the composition of raw materials selected for preparation of glass. When the temperature is lowered below  $T_g$ , the response time for molecular rearrangement becomes much larger than experimentally accessible times, so that liquid like mobility disappears and the atomic configuration becomes frozen into a set of fixed positions to which the atoms are tied. Possible range of glass formation is represented by temperatures  $T_{ga}$  and  $T_{gb}$ .  $T_{ga}$  is the glass transition temperature for a glass formed when the cooling rate is reduced and  $T_{gb}$  is that of increased rate of cooling. The

slopes of crystal and glass lines in a V-T diagram are small, compared to the high slope of the liquid section, which reflects the fact that the coefficient of thermal expansion of a solid is small in comparison with that of the liquid. An important change, the jump of heat capacity, also happens during liquid-glass transition, which is why physicists thought there is some sort of a phase transition, between the liquid phase and the glass phase.

## **Characterization techniques**

### **X-ray powder diffraction**

X-rays are electromagnetic radiation of wavelength about 1 Å, which is about the same size as an atom. Max von Laue, in 1912, discovered that the crystalline substances act as three-dimensional diffraction gratings for X-ray wavelengths similar to the spacing of planes in a crystal lattice. X-ray diffraction is a most common technique for the study of crystal structures and atomic spacing. Each crystalline solid has its unique characteristic X-ray powder diffraction pattern, which can be used as a "fingerprint" for its identification. Once the material has been identified, X-ray crystallography may be used to determine its structure, average particle size, unit cell dimensions and sample purity.

### **Principle**

X-ray powder diffraction is based on constructive interference of monochromatic X-rays and a crystalline sample. These X-rays are generated in a cathode ray tube by heating a filament to produce electrons, accelerating the electrons toward a target by applying a voltage, and bombarding the target material with electrons. When electrons have sufficient energy to dislodge inner shell electrons of the target material, characteristic X-ray spectra are produced. Copper is the most common target material for single-crystal diffraction, with  $\text{CuK}\alpha$  radiation = 1.5418 Å. The interaction of the incident rays with the sample produces constructive interference (and a diffracted ray) when conditions satisfy Bragg's Law ( $n\lambda = 2d \sin\theta$ ). Where 'n' is an integer referring to the order of reflection, 'λ' is the wavelength, 'd' is the spacing between the crystal lattice planes responsible for particular diffracted beam and 'θ' is the angle that incident beam makes with lattice planes. The path difference between the incident beam and the reflected beam in the consecutive lattice planes is shown in Fig. 3. The width of the Bragg's reflection in a standard X-ray powder diffraction pattern can provide information on the average grain size. The peak breadth increases as the grain size decreases, because of the reduction in the coherently diffracting domain size, which can be assumed to be equal to the average crystallite size. However, the average particle size can be estimated by using Scherrer's relation (1).

$$D = K\lambda/\beta \cos \theta \quad \dots(1)$$

where ' $\lambda$ ' is the X-ray wavelength, ' $\beta$ ' is the full width at half maximum of a diffraction peak, ' $\theta$ ' is the diffraction angle, and ' $K$ ' is the Scherrer's constant of the order of unity for usual crystal.

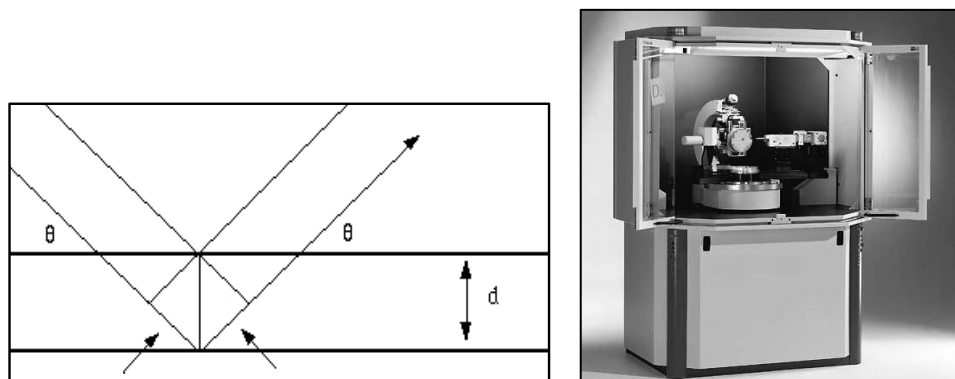


**Fig. 3: Schematic of photograph of X-ray diffractometer**

### **Fourier transform infrared (FT-IR) analysis**

Fourier transform spectroscopy is a simple mathematical technique to resolve a complex wave into its frequency components. The conventional IR spectrometers are not of much use for the far IR region, as the sources are weak and the detectors are insensitive. FT-IR made this energy-limited region more accessible. It also made the mid-infrared ( $4000\text{-}400\text{ cm}^{-1}$ ) more useful. In the fourier transform spectrometer, a time domain plot is converted into a frequency domain spectrum. The actual calculation of the Fourier transform of such systems is done by means of high-speed computers.

### **EXPERIMENTAL**

The FT-IR spectrometer consists of an infrared source, a sample chamber with a provision for holding solids, liquids and gases, monochromator, a detector and a recorder, which are integrated with a computer. At present, all commercially available infrared spectrophotometers employ reflection gratings rather than prisms as dispersing elements. Interferometric multiplex instruments employing the Fourier transform are now finding more general applications in both qualitative and quantitative infrared measurements. The interference pattern is obtained from a two-beam interferometer, as the path difference between the two beams is altered and then Fourier transformed output gives rise to the spectrum. The schematic diagram of a FTIR spectrometer is shown in Fig. 4. This instrument has resolution of  $0.1\text{ cm}^{-1}$ .

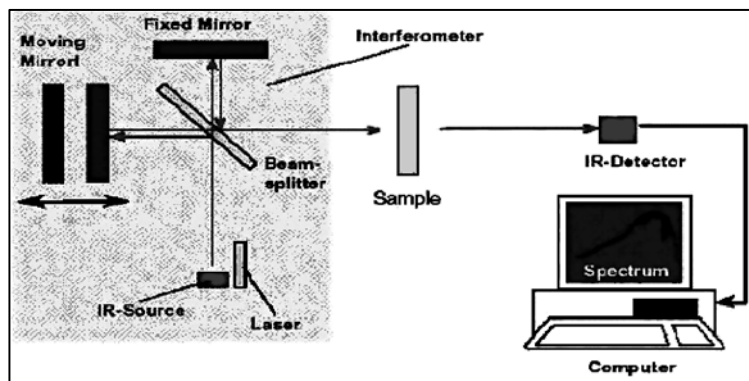


**Fig. 4: Schematic diagram of a FT-IR spectrometer**

Signal averaging, signal enhancement, baseline correction and other spectra manipulations are possible with multitasking OPUS software on the dedicated PC/AT 486. Spectra are plotted on a HP plotter and data can be printed. The recording of IR spectra of solid sample is more difficult because the particles reflect and scatter the incident radiation and therefore transmittance is always low. A few milligram of the sample is mixed with about 100 times the quantity of KBr which is transparent to the infrared using mullitemortar. The powder is pelletized in proper form suitable for IR transmission.

### UV-Vis-NIR spectroscopy

The experimental arrangement of Varian Cary 5E UV-Vis-NIR Spectrophotometer is shown in Fig. 5. UV-Vis-NIR spectroscopy is defined as the measurement of the absorption or emission of radiation associated with changes in the spatial distribution of electrons in atoms and molecules. In practice, the electrons involved are usually the outer valence or bonding electrons, which can be excited by the absorption of UV or visible or near IR radiation.

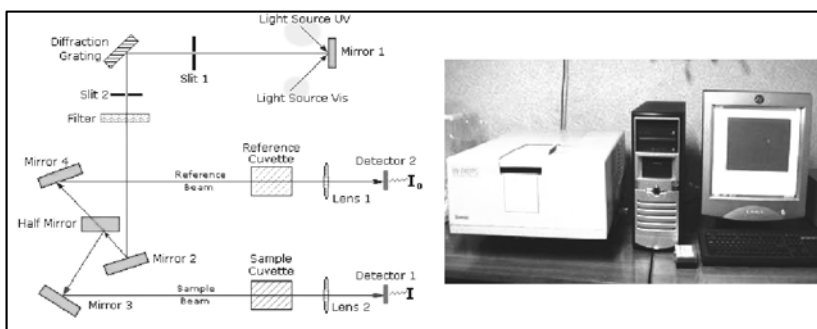


**Fig. 5: Schematic diagram and photograph of UV-Vis-NIR Spectrophotometer**

## Electronic energy levels and electronic transitions

Absorption of ultraviolet radiation by a molecule leads to electronic excitation among various energy levels within the molecule. The transitions generally occur in between a bonding or lone-pair orbital and an unoccupied non-bonding or anti-bonding orbital. The  $\sigma$  orbitals, involved in forming  $\sigma$  bonds, are the lowest energy occupied molecular orbitals. The  $\pi$ -orbitals lie at somewhat higher energy and the orbitals holding the unshared electron pairs (non-bonding orbitals) lie at even higher energy levels than the  $\pi$ -orbitals. The unoccupied or anti-bonding orbitals ( $\pi^*$  and  $\sigma^*$ ) are the orbitals of highest energy. The probability for electronic transitions determines the intensity of spectral lines. There must be large overlap between the vibrational states in the initial and the final electronic states to have a large absorption cross-section, or high probability that the molecule will absorb/emit radiation. Electronic transitions are possible for a wide range of vibrational levels within the initial and final electronic states. Saturated hydrocarbons and compounds containing only alkyl groups, alcohol groups and ether groups are transparent in the region 200-1000 nm. Such compounds are useful as solvents for making solutions of the specimen to study in this region. An isolated functional group not in conjugation with any other group is said to be a chromophore if it exhibits absorption of a characteristic nature in the ultraviolet or visible region. If a series of compounds have the same functional group and no complicating factors are present, all of them will generally absorb at very nearly the same wavelength. Thus, it is readily seen that the spectrum of a compound, when correlated with data from the literature for known compounds, can be a very valuable aid in determining the functional groups present in the molecule.

## Optical properties of glass

For each wavelength of light passing through the spectrometer, the intensity of the light passing through the reference cell is measured ( $I_0$ ). The intensity of the light passing through the sample cell is also measured for that wavelength ( $I$ ). If  $I$  is less than  $I_0$ , then obviously the sample has absorbed some of the light. For reasons to do with the form of the Beer- Lambert Law<sup>10</sup>, the relationship between  $A$  (the absorbance) and the two intensities are given by:

$$A = \log_{10} \frac{I_0}{I} \quad \dots(2)$$

The absorption coefficient,  $\alpha = A/d$ ,  $d$  = thickness of the sample. Generally, the absorption edge of these glasses is determined by the oxygen bond strength in the glass-forming network. Any change of oxygen bonding in the glass network, for instance, changes the formation of non bridging oxygen, thereby changing the characteristic absorption edge. For glasses and amorphous materials  $\alpha$  is given by the Tauc<sup>11,12</sup>,  $s$  relation,

$$\alpha(\omega) = B \left( \hbar\omega - E_{\text{opt}} \right)^{n/\hbar\omega} \quad \dots(3)$$

where, B is a constant and n is an index which takes values of 2, 1/2 for indirect and direct transitions. Band gap of glasses are calculated for indirect transitions, using Tauc plot, with  $(\alpha h\nu)^{1/2}$  along y-axis and  $E_{\text{opt}}$  along x-axis.

### **Refractive index (RI) measurement**

Refractive index is a measure of the distortion of atomic electron clouds by the electromagnetic field of an external incident light beam. Refractive index for a particular transparent medium is the ratio of the speed of light in one media compared to another, mathematically expressed as  $n_i = v_1 / v_2$ , where refractive index =  $n_i$  at a specific wavelength  $i$ , and the speed of light in each media are  $v_1$  and  $v_2$ . For glass analysis,  $v_1$  is the speed of light in a vacuum. Refractive indices were determined from the band gap<sup>13-16</sup>.

$$\left( \frac{n^2 - 1}{n^2 + 1} \right) = 1 - \sqrt{\frac{E_g}{20}} \quad \dots(4)$$

Refractive index can be calculated from the measured Brewster angle, which is related to refractive index as<sup>17</sup>–

$$n = \tan \theta_B \quad \dots(5)$$

### **Thermal studies**

#### **Introduction**

Recent trends indicate that thermal analysis has become well established method in the study of the thermal behaviour of materials and finds widespread applications in diverse industrial and research fields. Thermal analysis is a general term, which covers a group of related techniques in which the temperature dependence of the parameters of any physical property of a substance is measured. Thermal studies not only provide valuable information on the thermal stability of the compounds and the decompositions products but also provide an insight into their modes of decomposition.

#### **Thermoanalytical methods**

Thermoanalytical methods involve the measurement of various properties of materials subjected to dynamically changing environments under predetermined conditions of heating rate, temperature range and gaseous atmosphere or vacuum. Among the thermal



methods, the most widely used techniques are Thermogravimetry (TG), Differential thermal analysis (DTA) and Differential scanning calorimetry (DSC), which find extensive use in all fields of inorganic and organic chemistry, metallurgy, mineralogy and many other areas. In many cases, the use of a single thermoanalytical technique may not provide sufficient information to solve the problem on hand and hence the use of other thermal techniques, either independently or simultaneously for complementary information becomes necessary. For example, both differential thermal analysis (DTA) and thermogravimetry (TG) are widely used in studies involving physicochemical changes accompanied by variation in the heat content and the weight of the material.

### **Differential thermal analysis**

Differential thermal analysis (DTA) though, often considered an adjunct to TG, is in fact, far more versatile and yields data of a considerably more fundamental nature. The technique is simple as it involves the measurement of the temperature difference between the sample and an inert reference materials, as both are subjected to identical thermal regimes, in an environment heated or cooled at a constant rate. The origin of the temperature difference in the sample lies in the energy difference between the products and the reactants or between the two phases of a substance. This energy difference is manifested as enthalpic changes, either exothermic or endothermic. The differential thermal curve would be parallel to the temperature (time) axis till the sample undergoes any physical or chemical change of state. However, as soon as the sample has reached the temperature of this change of state, the additional heat flux reaching the sample will not increase the sample temperature at the same rate as that of the reference and the differential signal appear as a peak. The differential signal would return to the base line only after the change of state of the sample is completed and the temperature becomes equal to that of the reference material. The thermal effects are observed as peaks whose sequence, sign (endothermic or exothermic), magnitude and shape reflect the physical or chemical changes that take place. Since any change in the chemical or physical state of a substance is accompanied by changes in energy which are manifested as heat changes, the DTA method is applicable to all the studies listed for TG and also to phase transformations including polymerization, phase equilibrium and chemical reactions.

### **Thermal annealing**

Annealing is the process of reducing residual strain in glass by controlled heating and cooling. Annealing, in metallurgy and materials science, is a heat treatment wherein a material is altered, causing changes in its properties such as hardness and ductility. It is a process that produces conditions by heating to above the critical temperature, maintaining a

suitable temperature, and then cooling. Annealing is used to induce ductility, soften material, relieve internal stresses, and refine the structure by making it homogeneous. In the cases of copper, steel, silver, and brass, this process is performed by substantially heating the material (generally until glowing) for a while and allowing it to cool, so that it is softened and prepared for further work such as shaping, stamping, or forming. Annealing occurs by the diffusion of atoms within a solid material, so that the material progresses towards its equilibrium state. Heat is needed to increase the rate of diffusion by providing the energy needed to break bonds. The movement of atoms has the effect of redistributing and destroying the dislocations in metals and (to a lesser extent) in ceramics. This alteration in dislocations allows metals to deform more easily, so increases their ductility. The amount of process-initiating Gibbs free energy in a deformed metal is also reduced by the annealing process. In practice and industry, this reduction of Gibbs free energy is termed stress relief. The relief of internal stresses is a thermodynamically spontaneous process; however, at room temperatures, it is a very slow process. On annealing, mechanical properties, such as hardness and ductility, change as dislocations are eliminated and the metal's crystal lattice is altered. On heating at specific temperature and cooling, it is possible to bring the atom at the right lattice site and new grain growth can improve the mechanical properties.

### **Microhardness studies**

Hardness is an important factor in the choice of ceramics for abrasives, bearings, tool bits, wear resistance coatings etc. Hardness is a measure of resistance against lattice destruction or the resistance offered to permanent deformation or damage. Measurement of hardness is a destructive testing method to determine the mechanical behaviour of the materials. As pointed out by Shaw<sup>18</sup>, the term hardness is having different meanings to different people depending upon their areas of interest. For example, it is the resistance to penetration to a metallurgist, the resistance to cutting to a machinist, the resistance to wear and tear to a lubrication engineer and a measure of flow of stress to a design engineer. All these actions are related to the plastic stress of the material. For hard and brittle materials, the hardness test has proved to be a valuable technique in the general study of plastic deformation<sup>19</sup>. The hardness depends not only on the properties of the materials under test but also largely on the conditions of measurement. The microhardness method is widely used for studying the individual structural constituent elements of metallic alloys, minerals, glasses, enamels and artificial abrasives.

### **Vickers test**

Vickers test is said to be a more reliable method of hardness measurement. In order to get similar geometrical impression under varying loads, Smith and Sandland<sup>20</sup> suggested

that a pyramid at tip substituted for a ball. The Vickers hardness test method consists of indenting the test material with a diamond indenter, in the form of a right pyramid with a square base and an angle of  $136^\circ$  between opposite faces subjected to a load of 1 to 100 Kg (Fig. 6).

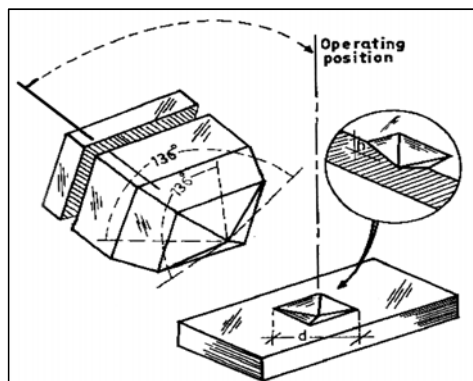


**Fig. 6: Vickers hardness test**

The base of the Vickers pyramid is a square and the depth of indentation corresponds to  $1/7^{\text{th}}$  of the indentation diagonal. The longitudinal and transverse diagonals will be in the ratio 7:1. The full load will be normally applied for 10 to 15 secs. The two diagonals of the indentation left in the surface of the material after removal of the load will be measured using a microscope and their average will be calculated. The area of the sloping surface of the indentation was calculated. The Vickers hardness is the quotient, which is obtained by dividing the kg load by the square mm area of indentation.

$$H_v = 1.8544 \left( \frac{P}{d^2} \right) \text{Kg/mm}^2 \quad \dots(6)$$

where  $H_v$  = Vickers hardness number

$P$  = Load in kg and

$d$  = Arithmetic mean of the two diagonals

When the mean diagonal of the indentation has been determined, the Vickers hardness number can be calculated from the above formula. The several different loading settings give practically identical hardness numbers on uniform material, which is much better than the arbitrary changing of scale with the other hardness testing methods. The advantages of the Vickers hardness test are that extremely accurate readings can be taken, and just one type of indenter is used for all types of metals and surface treatments.

### **Knoop hardness studies**

Knoop hardness can be treated as an alternative to the Vickers test, particularly for very thin layers, Fredrick Knoop developed a low-load test with a rhombohedral-shaped diamond indenter. The long diagonal is seven times (7.114 actually) as long as the short diagonal. With this indenter shape, elastic recovery can be held to a minimum. Knoop tests are mainly done at test forces from 10 g to 1000 g (Fig. 7), so a high powered microscope is necessary to measure the indent size. Because of this, Knoop tests have mainly been known as microhardness tests. The magnifications required to measure Knoop indents dictate a highly polished test surface.

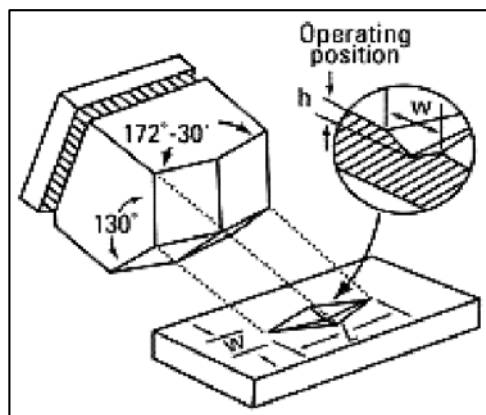


**Fig. 7: Knoop hardness test**

### **Dielectric studies**

The useful method of characterization of electrical response is the dielectric studies. The frequency dependence of these properties gives great insight into the materials applications. The range of measurement depends on the properties and the materials of interest. From the study of dielectric constant as a function of frequency, temperature etc., the different polarization mechanisms in solids such as atomic polarization of the dipoles, space-charge polarization etc., can be understood.

### **Experimental setup**

The suitably cut and polished samples (with known dimensions) of grown crystals subjected to dielectric studies by using HIOKI 3532-50 HITESTER LCR meter (Fig. 8) with a conventional four terminal sample holder for investigations involving temperature

variations and a conventional two terminal sample holder (Westphal) for only ambient conditions. The samples are prepared and mounted between copper platforms and electrodes. In order to ensure good electrical contact, the glass faces are coated with the silver paint. The capacitance and the dissipation factor of the parallel plate capacitor formed by the copper plate and the electrode having the sample as a dielectric medium are measured. The dielectric constant and dielectric loss are calculated using the equations 9 and 13, respectively. The measurements are made at frequencies ranging from 50Hz to 5MHz at different temperatures.

### Dielectric constant

One of the most important parameters widely used is the dielectric constant or relative permittivity. The dielectric constant of a material may be defined as the ratio of the field strength in vacuum to that in the material for the same distribution of charge. The dielectric constant of a substance is a property of the constituent ions. In general, if electrode effects are neglected, the four major components contributing to the dielectric constant are:

- (i) Extrinsic nature of the material,
- (ii) Electronic polarizability,
- (iii) Ionic polarizability and
- (iv) Deformation of the ions.

The dielectric constant or relative permittivity can be defined as,

$$\epsilon_r = \frac{\epsilon}{\epsilon_0} \quad \dots(7)$$

We know that

$$\epsilon = \frac{Cd}{A} \quad \dots(8)$$

Thus, we have

$$C = \epsilon_r \epsilon_0 A / d \quad \dots(9)$$

where  $A$  is the area of the sample,  $d$  is the thickness of the sample. The relative permittivity ( $\epsilon_r$ ) is usually known as dielectric constant. It is always greater than unity.

Suppose a parallel plate condenser has a capacitance of  $C_0$  in air then its capacitance when the space between the plates is filled by a medium of dielectric constant  $\epsilon_r$  is given by,

$$C = C_0 \epsilon_r$$

$$\epsilon_r = \frac{C}{C_0} \quad \dots(10)$$

$\epsilon_r$  can be found out from the measurement of capacitance. The dielectric constant in any direction of the medium can be considered as a measure of electrostatic binding strength between the ions in the direction. The higher the dielectric constant, the lower the electrostatic binding and hence higher is the lattice energy.

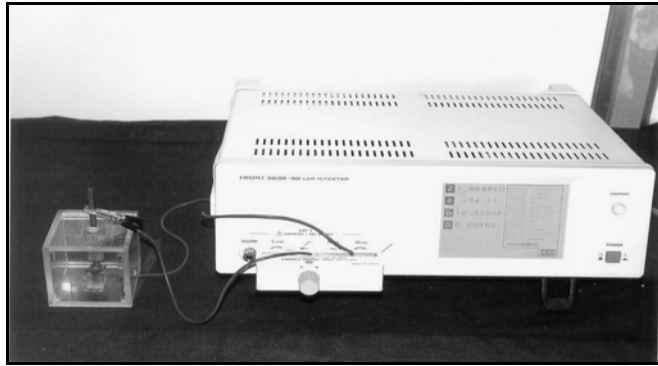


**Fig. 8: Photograph of HIOKI 3532-50 LCR HITESTER**

### Dielectric loss

When a dielectric is subjected to an alternating electric field, the electric field strength changes as,

$$E = E_0 \cos \omega t \quad \dots(11)$$

The induced current in the dielectrics does not change exactly with the applied voltage. The current is found to lead the potential in phase. In a similar way, the electrical displacement is also not in phase with respect to  $E$ . Now the expression for  $D$  becomes,

$$D = D_0 \cos (\omega t - \delta)$$

$$D = D_0 \cos \omega t \cos \delta + D_0 \sin \omega t \sin \delta \quad \dots(12)$$

The factor  $\sin \delta$  is a measure of the energy absorbed by dielectrics. It is known that in a capacitor the dielectrics usually have a resistance  $R$  and impedance  $Z$  that are related to the phase angle. Assuming  $R$  to be very large,

$$\sin \delta \approx \tan \delta = 1/\omega RC \quad \dots(13)$$

The factor  $\tan \delta$  is referred to as the dielectric loss.

### **Fluorescence spectroscopy**

Optical fluorescence of glasses was carried out using Cary Eclipse Fluorescence spectrophotometer of VARIAN<sup>21</sup>. It has a single cell holder for liquid sample analysis and a solid sample holder accessory to perform fluorescence measurements on solid samples. The solid sample holder accessory provides both rotational and translational adjustment of the sample. The angle of incidence of the excitation may be varied from 20-35°C. This is the angle between the exciting light and a line perpendicular to the surface of the sample mounting slide. The source of excitation is xenon lamp.

### **Laser induced fluorescence spectroscopy**

Laser induced photoluminescence is spontaneous emission from atoms or molecules that have been excited by laser radiation. Two radiative transitions are involved in the Laser induced photoluminescence process. First, absorption takes place, followed by a photon-emission. Laser induced photoluminescence is a dominant laser spectroscopic technique in probing of unimolecular and bimolecular chemical reactions. This technique serves as a sensitive monitor for the absorption of laser photons in fluorescence excitation spectroscopy. It is well suited to gain information on molecular states if the fluorescence spectrum excited by a laser on a selected absorption transition is dispersed by a monochromator. Experimental set up for Laser induced luminescence is shown in Fig. 9. The pump beam is taken from a Quanta Ray Q-switched Nd: YAG laser which emits pulses of 7 ns duration at 532 nm and 355 nm, at a repetition rate of 10 Hz. A cylindrical lens is used to focus the pump beam in the shape of a stripe on the sample. In the present case it is adjusted to a pump beam width of 7 mm. The output is collected from the edge of the front surface of the sample using an optical fiber in a direction normal to the pump beam. The emission spectra are recorded with Acton monochromator attached with a CCD camera. Princeton Instruments NTE/CCD air cooled detectors have three distinct sections. The front vacuum enclosure contains the CCD array seated on a cold finger. This finger is in turn seated on a four-stage Peltier thermoelectric cooler. The back enclosure contains the heat exchanger. An internal fan cools the heat exchanger and the heat exits the unit through openings in the housing.

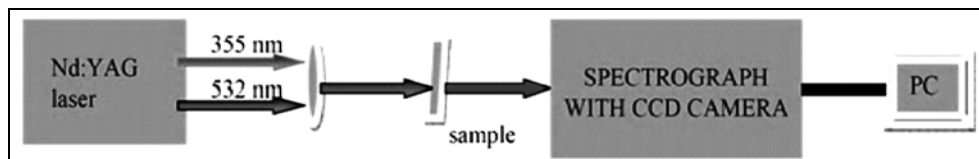


**Fig. 9: Experimental set up of Laser induced luminescence**

### Nonlinear optical characterization

Recent interest is focused on to find the materials, which have suitable nonlinear optical properties for use as the active media in efficient second harmonic generators, tunable parametric oscillators and broadband electro-optic modulators. Kurtz and Perry<sup>22</sup> proposed a powder SHG method for comprehensive analysis of the second order nonlinearity. By employing this technique, Kurtz surveyed a very large number of compounds.

### Experimental setup

The nonlinear optical property of a material can be tested by passing the output of Nd: YAG Quanta ray laser. The schematic of the experimental setup used for SHG studies is shown in Fig. 10.

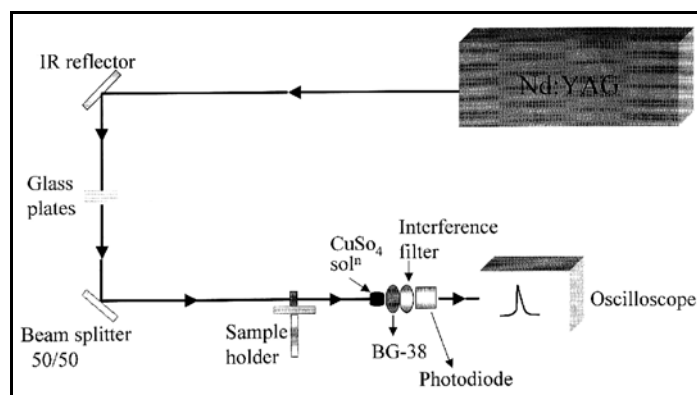


**Fig. 10: Schematic experimental setup for SHG efficiency measurement**

A Q-switched, mode locked Nd: YAG laser will be used to generate about 6 mJ/pulse at the 1064 nm fundamental radiation. This laser can be operated in two modes. In the single shot mode, the laser emits a single 8 ns pulse. In the multi shot mode, the laser produces a continuous train of 8 ns pulses at a repetition rate of 10 Hz. In the present study, a single



shot mode of 8 ns laser pulse with a spot radius of 1 mm is used. The experimental setup uses a mirror and a 50/50 beam splitter (BS) to generate a beam with pulse energies about 6.2 mJ. The input laser beam is allowed to pass through an IR reflector and then directed on to the micro crystalline powdered sample packed in a capillary tube of a diameter 0.154 mm. The light emitted by the sample is measured by the photodiode detector and oscilloscope assembly.

### Z-scan technique

There are a number of techniques for measuring the optical nonlinearity exhibited by semiconductors such as degenerate four wave mixing, optical Kerr effect, ellipse rotation, interferometric methods etc. The z-scan technique was invented by Shiehe Bahae et al.<sup>23</sup>. It has many advantages over other nonlinear measurement techniques that it is simple, very sensitive and fast, giving the sign of optical nonlinearity immediately. There are closed and open aperture z-scan; the former is sensitive to both nonlinear absorption and refraction and the latter is sensitive to only nonlinear absorption. Fig. 11 shows the experimental set up of z-scan technique.

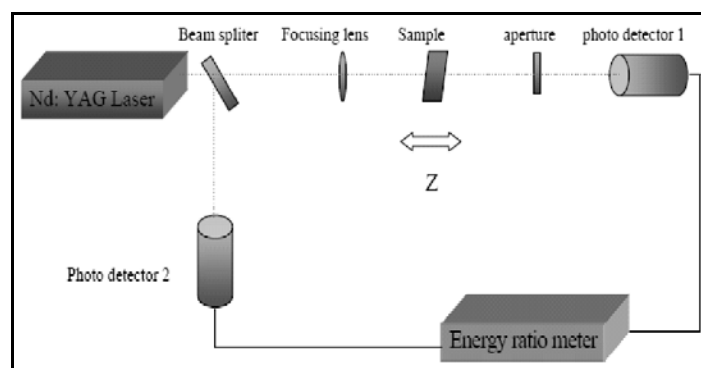


**Fig. 11: Experimental set up of z scan technique**

A Q-switched Nd: YAG laser (Spectra Physics LAB-1760, 532 nm, 7 ns, 10 Hz) is used as the light source. The sample is moved in the direction of the light incidence near the focal spot of the lens with a focal length of 20 cm radius of the beam waist  $\omega_0$  is calculated to be 42.56  $\mu\text{m}$ . The Rayleigh length,  $z_0 = \pi\omega_0^2/\lambda$ , is estimated to be 10.06 mm, much greater than the thickness of the sample, which is an essential prerequisite for z-scan experiments. The transmitted beam energy, reference beam energy, and their ratio are measured simultaneously by an energy ratio meter (Rj7620, Laser Probe Corp.) having two identical pyroelectric detector heads (Rjp735). The sample was moved along the z-axis by a

motorized translational stage. At the focus the power output of the laser beam was measured in  $\text{GW}/\text{cm}^2$ . The z-scan system is calibrated using carbon disulphide, which is taken as a standard nonlinear material. The effect of fluctuations of laser power is eliminated by dividing the transmitted power by the power obtained at the reference detector. Z-scan technique is highly sensitive to the profile of the beam and also to the thickness of the sample. Any deviation from gaussian profile of the beam and also from thin sample approximation will give rise to erroneous results. For ensuring that the beam profile does not vary appreciably inside the sample, the sample thickness should always be kept less than the Rayleigh's range. The sensitivity of this z-scan method is used to monitor nonlinear refraction at low irradiance levels, where a third order nonlinearity attributed to  $n_2$  caused by bound electrons can be observed. At higher irradiance levels the refraction caused by two photon absorption induced free charge carriers becomes significant.

### **Thermal poling**

Second-order nonlinear (SON) optical properties are forbidden in glasses, which exhibit inversion symmetry on a macroscopic scale. However, it is possible to induce a second-order nonlinear susceptibility in bulk glass using specific treatment like optically assisted poling or thermal poling<sup>24-29</sup>. Among them, thermal poling that applies dc voltage at high temperature is most commonly used. Glasses are one among the oxide/chalcogenide glasses, which are finding a number of applications due to their properties such as high refractive index, low phonon energy, low transition temperature, excellent infrared transmission and very high optical nonlinearities. The purpose of thermal poling in this thesis is to investigate its effect on the optical properties of glass samples. Glass samples for the present work were synthesized by rapid melting quenching method. These samples were polished using various grades of silicon carbide powder for obtaining parallel, smooth and clear surface for experiment. The thickness of the glass specimens was measured using a digital micrometer gauge. Thermal poling measurements were carried out by the setup shown in Fig. 12. The poling was performed on 1.3 mm thick samples placed in between two flat electrodes made of stainless steel.

The glass sample sandwiched between the electrodes were put into a furnace and heated to an aimed temperature from 100-300°C. After holding the samples at a temperature for 30 mins, an electric field 1-2 kV was applied. The temperature was then decreased to room temperature while the voltage was held a constant. The applied dc field was removed after the sample reached the room temperature. Maximum temperature range for thermal poling is limited to the glass transition temperature. Absorption spectra were taken before and after thermal poling.

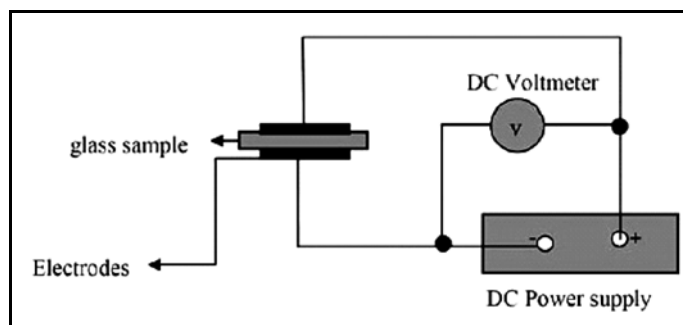


**Fig. 12: Experimental set up of thermal poling**

## CONCLUSION

This review discusses the preparation and characterization techniques for melt quenched glass used in the research work. The structural characterization techniques used such as powder XRD, FT-IR and UV-Vis-NIR spectral, thermal, hardness, dielectric, measurements are discussed in detail. Photoluminescence studies of glasses carried out using Fluorescence spectrophotometer are also discussed. The major experimental tools used for the study are Z-scan technique for nonlinear characterization of the sample, thermal poling to tune the linear and non linear optical properties of glasses and Laser Induced Fluorescence spectroscopy to probe into the defect states of these glasses.

## ACKNOWLEDGEMENT

The author would like to thank the Board of Research in Nuclear Sciences (BRNS) for funding this major research project.

## REFERENCES

1. Masayuki Yamane and Yoshiyuki, Glasses for Photonics, Cambridge University Press, Spain (2000).
2. Valentina Kokorina, Glasses for Infrared Optics, CRC Press, Boca Raton, Fla (1996).
3. M. R. Sahar, K. Sulhadi and M. S. Rohani, Mater Sci, **42**, 824-827 (2007).
4. E. M. Vogel, J. Am. Ceram. Soc., **72**, 719 (1989).
5. A. A. Sidek, S. Rosmawati, Z. A. Talib, M. K. Halimah and W. M. Daud, Am. J. Applied Sci., **6(8)**, 1489-1494 (2009).

6. A. H. Raouf, El-Mallawany, Tellurite Glasses Handbook, Physical Properties and data, CRC Press LLC (2002).
7. D. Adler, Amorphous Semiconductors, CRC Press, Boca Raton, FL, **5** (1971).
8. W. Vogel, Chemistry of glasses, American Ceramics Society, Westerville, OH (1985).
9. Arun K. Vashneya, Fundamentals of Inorganic Glasses, Accademic Press Inc. (1994).
10. Infrared Spectroscopy: Theory, Online Edition for Students of Organic Chemistry Lab Courses at the University of Colorado, Boulder, Dept. Chem. Biochem. (2002).
11. N. F. Mott and E. A. Davis, Conduction in Non-Crystalline Systems V. Conductivity, Optical Absorption and Photoconductivity in Amorphous Semiconductors, Philos. Mag., **28**, 903 (1970).
12. H. Burger, K. Kneipp, H. Hobert and W. Vogel, J. Non-Cryst. Solids, **151**, 134-142 (1992).
13. B. Erariah, Bull. Mater. Sci., **33**, 391-394 (2010).
14. R. El-Mallawany, M. Dirar Abdalla and I. Abbas Ahmed, Mater. Chem. Phys., **109**, 291-296 (2008).
15. V. Dimitrov and S. Sakka, J. Appl. Phys., **79**, 1736 (1996).
16. P. Gayathri Pavana, K. Sadhanab and V. Chandra Mouli, Physica B, **406**, 1242-1247 (2011).
17. H. E. Bennett, J. M. Bennett, W. G. Driscoll and W. Vaughan, "Polarization," in Handbook of Optics, Eds. McGraw-Hill, New York, 10-1 to 10-164 (1978).
18. M. C. Shaw, The Science of Hardness Testing and its Research Application, Ed. By J. H. Westbrook and H. Conrad, ASM. Ohio (1973) pp. 1-11.
19. J. H. Westbrook and H. Conrad, The Science of Hardness Testing and its Research Applications, Am. Soc. Met., Ohio (1971).
20. R. L. Smith and G. E. Sandland, An Accurate Method of Determining the Hardness of Metals with Reference to those of a High Degree of Hardness, Proc. Inst. Mech. Engrs., **1**, 623-641 (1923).
21. Cary Eclipse Hardware Operation Manual, VARIAN, Australia (2000).
22. S. K. Kurtz and T. T. Perry, J. Appl. Phys., **39**, 3798-3813 (1968).
23. Mansoor Sheike Bahae, Ali A. Said, Tai-Huei Wei, David J. Hagan, E. W. Van Stryland, IEE J. Quant. Electron., **26**, 760-769 (1990).

24. R. A. Myers, N. Mukherjee and S. R. J. Brueck, *Opt. Lett.*, **16**, 1732 (1991).
25. N. Mukherjee, R. A. Myers and S. R. J. Brueck, *J. Opt. Soc. Am. B*, **11**, 665 (1994).
26. P. G. Kazansky, V. Pruneri and P. St. J. Russell, *Opt. Lett.*, **20(8)**, 843 (1995).
27. L. J. Henry, A. D. DeVilbiss and T. E. Tsai, *J. Opt. Soc. Am. B*, **12**, 2037 (1995).
28. H. Nasu, H. Okamoto, K. Kurachi, J. Matsuoka, K. Kamiya, A. Mito and H. Hosono, *J. Opt. Soc. Am. B*, **12**, 644 (1995).
29. T. Fujiwara, M. Takahashi and A. Ikushima, *Appl. Phys. Lett.*, **71(8)**, 1032 (1997).

*Revised : 12.03.2015*

*Accepted : 15.03.2015*